Lattice relaxation in many-electron states of the diamond vacancy

M. Heidari Saani,[1,2] M. A. Vesaghi,[1] K. Esfarjani,[1] T. Ghods Elahi,[1,3] M. Sayari,[1] H. Hashemi,[1] and N. Gorjizadeh[1]
[1]*Department of Physics, Sharif University of Technology, Tehran, P. O. Box 11365-9161, Iran*
[2]*Semiconductor Component Industry, Tehran, P. O. Box 19575-199, Iran*
[3]*Institute for Studies in Theoretical Physics and Mathematics (IPM), School of Physics, Tehran, P. O. Box 19395-5531, Iran*
(Received 6 June 2004; revised manuscript received 15 September 2004; published 5 January 2005)

Symmetric lattice relaxation around a vacancy in diamond and its effect on many electron states of the defect have been investigated. A molecular approach is used to evaluate accurately electron-electron (*e*-*e*) interaction via a semiempirical formalism which is based on a generalized Hubbard Hamiltonian. Coupling of the defect molecule to surrounding bulk is also considered using an improved Stillinger-Weber potential for diamond. Strong dependence of the electronic energy levels to the relaxation size of the nearest neighbor (NN) atoms indicates that in order to obtain quantitative results the effect of lattice relaxation should be considered. Except for the high spin state of the defect $^5A_2$, the order of other lowest levels, particularly the ground state of the vacancy ^1E does not change by the relaxation. At 12% outward relaxation, there is a level crossing between $^5A_2$ and the excited state of the well-known GR1 transition $^1T_2$. The reported level crossing confirms the predicted relative energies of these states in the band gap that was speculated by monitoring the temperature dependence of the electron paramagnetic resonance (EPR) signal. By considering the outward relaxation effect, we obtained midgap position for the $^5A_2$ state in agreement with the suggestion made by EPR. The position of the low lying $^3T_1$ level varies from 100 to 400 meV with increasing outward relaxation. When the ion-ion interaction of the NN atoms is included the outward relaxation lowers the energies of all electronic states. The relaxing force is different for investigated electronic states. By considering the interaction of the first and second shell neighbors of the vacancy, the calculated elastic barrier restricts outward relaxation of the vacancy to 12% for the ground and 18% for the $^5A_2$ excited state. The calculated equilibrium bond lengths are in very good agreement with *ab initio* density functional theory and EPR measurement data. Electronic configurations in the unrelaxed and relaxed eigenfunctions of the Hamiltonian are reported. Our results also suggest that there is an outward relaxation if Hund rule is applicable.

DOI: 10.1103/PhysRevB.71.035202 PACS number(s): 61.72.Bb, 61.72.Ji, 71.55.−i

I. INTRODUCTION

For the past 50 years, lattice vacancy in diamond and more recently in silicon have been studied as the principal benchmark for the more general problem of deep levels in semiconductors.[1,2] The electron paramagnetic resonance (EPR) measurements and *ab initio* calculations suggest that the nearest neighbor (NN) atoms of the vacancy relax somehow. This effect is common for lattice vacancies in semiconductors and has been investigated widely both in theory and experiment. Qualitative results for the size and sign of the lattice relaxation comes out from hyperfine interaction (HFI) measurements of the EPR.[3,4] Theoretical calculations based on density functional theory (DFT) and within the local spin density approximation (LSDA) are used to predict the relaxation size[5,6] and to explain HFI experimental data.[7,8]

The sign of the relaxation is expected to be important in any elastic energy-barrier to interaction with another defect, as well as determining the perturbation of any defects that are near a vacancy.[9] In contrast to the vacancy in Si lattice, the lattice vacancy in diamond does not undergo Jahn-Teller distortion and the relaxation around the defect is expected to be symmetric.[10] The sign and size of relaxation in the ground state of the defect, is still in dispute.[9] *Ab initio* density functional theory calculations predicted 13% and 7% outward relaxation for NN atoms using a molecular cluster and a plane-wave-supercell, respectively[5,6] in agreement with original large cluster calculation results.[11] The complete neglect of differential overlap (CNDO) method gives up to 10% inward relaxation.[12] With a different set of parameters in CNDO, it is also possible to obtain outward relaxation.[12] Using an empirical Stillinger–Weber potential for C—C interaction gives 10% inward relaxation.[13] This sign of the relaxation is in agreement with original results of the molecular model introduced by Coulson and Larkins.[14] In all of the calculations the relaxation of the next nearest neighbor (NNN) atoms is negligible. The difference between these approaches essentially depends upon the treatment of *e*-*e* correlation.[13] Any elastic measurement of the phonon structure of the vacancy GR1 optical band indicates that elastic forces in the locality of the diamond vacancy were only marginally changed from those of the bulk material.[15] This implies that any elastic softening near the vacancy is relatively small.[13]

The ground state of the neutral vacancy ^1E is diamagnetic ($S=0$) and therefore was not studied by EPR. Our knowledge about the relaxation of this center comes out from EPR measurements[3] on a paramagnetic excited state of the neutral vacancy, i.e., $^5A_2$ and the following *ab initio* studies[7,8] of the HFI interaction parameters within the LSDA framework of DFT. Experimental results suggest that the relaxation in this excited state is 15% and outward.[3] Hund rule is not valid for the vacancy and the ground state is not $^5A_2$. This has been attributed to the subtle *e*-*e* interaction in the diamond vacancy.[16] The EPR measurements also suggest negligible

lattice relaxation for the NNN atoms[17] in agreement with theoretical calculations.[5,13]

Despite many theoretical attempts that invesigate lattice relaxation in the ground state of the vacancy, there are very few works[14] that consider the relaxation effect on the multiplet electronic structure of the vacancy. Using the original molecular CI model,[1] Coulson and Larkins[14] examined the effect of lattice relaxation as a perturbation on the energies of unrelaxed states. Their approach assumed that the effect of lattice relaxation on many electron states is more important than the effect of Jahn-Teller distortion. The ion-ion (*i*-*i*) interaction was approximated by $F\Delta R$ expression for small displacement of the NN atoms (ΔR), where F is the symmetric relaxing force that was defined as the gradient of the energy expectation value in each electronic state. The elastic energy in harmonic regime, was considered as $\frac{1}{2}m\omega^2\Delta R^2$ where m is the mass of a carbon atom and ω is the effective phonon frequency of the lattice. These two terms were considered as the first and second order perturbation to the unrelaxed energies of the states. They obtained different symmetric relaxing force for different many electron states. However for all of the energy states in their model, the four NN atoms of the vacancy relax inward. As they discussed, an outward relaxation is more expected from the chemical point of view. In the extreme condition, while the methane molecule has three dimensional tetrahedral structure the methyl radical is planner. The outward relaxation leads to the atoms surrounding the vacancy moving more into the plane of their three nearest neighbors, and the bonding becoming more sp^2 like than sp^3, with the former being preferred.[5]

Extension of the CI calculation in its original form, to investigate lattice relaxation in many electron multiplet with an unperturbative formalism is too demanding. Additionally for the electronic systems such as diamond vacancy where many particle effects are dominant, local density approximation (LDA) is not able to describe *e*-*e* interaction adequately.

In this work, we use a semiempirical formalism based on a generalized Hubbard Hamiltonian in order to consider *e*-*e* interaction more accurately. The model considers the vacancy as an isolated molecule. To include the effect of surrounding bulk, the coupling of the defect NN atoms with the second neighbor shell of atoms (NNN) is considered. We use an improved SW interatomic potential for diamond to calculate the elastic energy of the NN-NNN bonds. In this calculation we assume that the variation of the SW potential with relaxation, mainly comes from the change of the distance between atoms. Since the empirical parameters reproduce the elastic and vibrational properties of diamond lattice, we assume that the parameter variation is negligible for small displacements. We obtained strong dependence of electronic energies on the size of the relaxation and different relaxing forces for the different states. The size and sign of the relaxation in each many electron state will be reported. By considering this effect, the puzzling of the midgap position for the $^5A_2$ state suggested by EPR, will be resolved. A level crossing between the $^5A_2$ and $^1T_2$ states at 12% outward relaxation is reported. Electronic configurations in the unrelaxed and relaxed states were calculated to explain the behavior of the electronic states under relaxation.

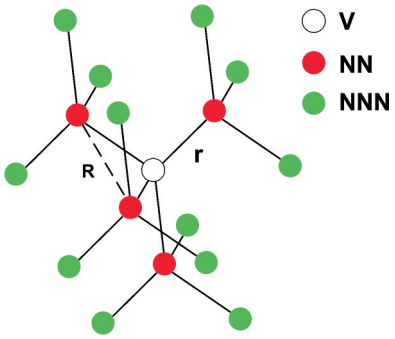

FIG. 1. (Color online) The lattice vacancy in diamond with its first (NN) and second (NNN) shell neighbors. The distance between NN atoms (R) in unrelaxed lattice is 2.52 Å and the radial distance from vacancy to the NN atoms (r) is 1.54 Å

II. CALCULATIONS

To find the effect of lattice relaxation on the total energy of a vacancy in the diamond lattice, we consider the total energy as a sum of electronic (*e*-*e*,*e*-*i*), ionic (*i*-*i*) and elastic (NN-NNN) energies in Eq. (1). Based on the EPR result,[3,4] we assumed that the displacements of the (NNN) atoms of the vacancy is negligible. Hence in this equation all energy terms of the lattice that change with relaxation around a vacancy are considered,

$$\Delta E_L = \Delta E_V(e\text{-}e) + \Delta E_V(e\text{-}i) + \Delta E_V(i\text{-}i) + \Delta E_V(\text{NN-NNN}) \tag{1}$$

In this equation ΔE_L is the change of the lattice energy due to relaxation around a vacancy. ΔE_V's are the change of the energy of a vacancy that consist of electron-electron, electron-ion, and ion-ion interaction energies. The last term is the change in the elastic energy due to the interaction of the NN with NNN atoms. It should be emphasized that the localized character of the relaxation effect around the vacancy that caused NNN atoms to be almost fixed, enabled us to write Eq. (1).

A. Calculation of electronic and ionic energies

We used a generalized Hubbard Hamiltonian, to calculate energy levels of electrons including electron-ion (*e*-*i*) and *e*-*e* interaction completely. The Hamiltonian can be factorized by using tetrahedral, T_d, symmetry of the vacancy,

$$H = t\sum_{ij,\sigma} c_{i\sigma}^{\dagger}c_{j\sigma} + U\sum_{i} n_{i\uparrow}n_{i\downarrow} + \frac{V}{2}\sum_{i\neq j,\sigma\sigma'} n_{i\sigma}n_{j\sigma'} + \frac{1}{2}\sum_{ijlm,\sigma\sigma'} X_{ijlm}c_{i\sigma}^{\dagger}c_{j\sigma'}^{\dagger}c_{m\sigma'}c_{l\sigma}, \tag{2}$$

i, j, l, and m are indices of dangling orbitals of the vacancy that are localized on the NN atoms in Fig. 1.

They range from 1 to 4. σ, σ' are the spin indices that take up and down values. $c_{i\sigma}$ and $c_{i\sigma}^{\dagger}$ are annihilation and creation operator for an electron on site i with spin σ, respectively. The $n_{i\uparrow}$ and $n_{i\downarrow}$ are spin occupation number operators

that act on site i. t is the single particle parameter that includes kinetic energy and electron-ion interaction. It is named as the on-site energy for $(i=j)$, and the hopping energy for $i \neq j$. U and V are Coulombic integrals that represent classical on site and interatomic e-e interaction terms, respectively. X_{ijlm} are exchange integrals that represent quantum correlations that reduce to $X_1, \ldots, X_5$ with tetrahedral symmetry of the defect. These parameters are defined as

$$t_{ij} = \langle i|T + V(r)|j\rangle,\ U = \langle ii|\frac{1}{r}|ii\rangle,\ V = \langle ij|\frac{1}{r}|ij\rangle,$$

$$X_1 = \langle ij|\frac{1}{r}|ji\rangle,\ X_2 = \langle ii|\frac{1}{r}|ij\rangle,\ X_3 = \langle ij|\frac{1}{r}|ik\rangle, \qquad (3)$$

$$X_4 = \langle ii|\frac{1}{r}|jk\rangle,\ X_5 = \langle ij|\frac{1}{r}|kl\rangle.$$

The parameters listed in Eq. (3) are calculated directly from atomic orbitals. Similar parameters in the previous molecular approach,[1] were calculated from molecular orbitals that were the symmetric (antisymmetric) linear combination of the atomic orbitals. The Slater-type functions are used in both approaches for atomic orbitals to calculate Hamiltonian parameters.[18]

Recent EPR experiments indicate that almost all of unpaired electrons of lattice vacancy in diamond are localized on the nearest neighbor atoms of the vacancy.[4] This implies that considering four dangling orbitals for calculating electronic structure properties is reasonable.[17] Details of the Hamiltonian calculation has been published elsewhere.[18]

Except for the on-site energies t_{ii} and U, all parameters in Eq. (3) are sensitive to the relative distance of the ions. t_{ii} and U are one center integrals that are independent of R. The hopping parameter t_{ij} is obtained from the on-site energy t_{ii} by $t_{ij}=s_{ij}t_{ii}$, where $s_{ij}=s$ is the overlap integral of ith and jth dangling orbitals and it is the same for all i and j. Dangling orbitals are localized on the NN atoms and by the symmetric outward or inward relaxation, the overlap integral of orbitals decreases or increases, respectively. We used the semiempirical value of 12.855 eV for the parameter U,[14] while its theoretically calculated value in the original molecular model is 19 eV.[1] The large difference between this semiempirical and the theoretical value was explained[18] by electron delocalization from NN atoms of the defect molecule to the NNN atoms of the lattice and the reported[10] deviation of the charge distribution from ideal sp^3 distribution. Other parameters of Eq. (3) are calculated with Slater-type orbitals.[18]

In calculating other multicenter integrals, the ionic distance R in Fig. 1, enters explicitly. For a reasonable range of the outward and inward lattice relaxation, we calculated the Hamiltonian parameters. The parameters were calculated by decreasing and increasing R (r) in the range -20% to $+30\%$ for the inward and outward relaxation, respectively. The steps of radial displacement (r) of atoms in this process were 2% or 0.031 Å. We obtained many electron energies and eigenfunctions for each set of parameters.

The first two terms of Eq. (1) have been calculated from the generalized Hubbard Hamiltonian of Eq. (2) and the ion-ion energy term has been calculated from Coulombic repulsion energy (e^2/R) between bare ions due to the relatively large distance between NN ions (2.52 Å).

B. Calculation of NN-NNN interaction energy

Symmetric displacement of the vacancy atoms also affects the elastic energy that comes from the bonds between the NN and NNN atoms [last term in Eq. (1)]. This introduces a limit to the amount of energy lowering of the vacancy molecule by relaxation. After calculation of the the e-e and e-i energies with respect to the relaxation, we used an appropriate interatomic potential to describe the energy of the NN-NNN interaction to obtain the final equilibrium position of the NN atoms in each electronic state.

A widely used potential for describing atomic interaction in covalent tetrahedrally bounded systems is the empirical potential derived by Stillinger and Weber.[19] Carbon is also represented by a number of empirical potentials that are called bond order such as those of Tersoff[20] and Brenner.[21] However if only sp^3 bonded clusters are under consideration, the SW potential should compare well with these bond order potentials and agrees well with the elastic and vibrational properties of diamond.[22] The SW potential has been previously used to investigate the relaxation effect around a vacancy in diamond.[13] In this work we used a recently improved form of this potential for diamond.[22,23] The empirical parameters were obtained through a fit to *ab initio* Hartree-Fock and MP2 methods and they produce properly bulk properties of diamond such as elastic and vibrational constants.[22,23] The form of the SW potential which includes two-body and three-body terms for an N atom system is as follows:

$$\frac{U}{\epsilon} = \sum_{i<j} U^{(2)}(r_{ij}/\sigma) + \sum_{i<j<k} U^{(3)}(r_i/\sigma, r_j/\sigma, r_k/\sigma), \qquad (4)$$

where $U^{(2)}$ and $U^{(3)}$ are the two-body and three-body interaction terms in reduced units, respectively.

The improved parameters for the diamond are[22,23]

$$A = 5.378\,9794, \quad B = 0.593\,3864,$$

$$\lambda = 26.199\,34, \quad \gamma = 1.055\,116,$$

$$a = 1.846\,285, \quad \epsilon(\text{eV}) = 3.551, \quad \sigma(\text{Å}) = 1.368.$$

In the above parameters, a is the cutoff radius of interaction that is 1.846 Å. Since the distances between NN and NNN atoms in the diamond lattice are 1.54 Å and 2.52 Å, respectively, this cutoff implies that in the SW potential, only the interaction between NN atoms is considered. This cutoff guarantees the independence of the electronic energy in Eq. (2) based on generalized Hubbard Hamiltonian, upon the elastic energy calculation for the NN-NNN bonds in the lattice with the SW potential. Therefore we can add the variation of the electronic and ionic parts of the energy to the variation of the calculated elastic energy from Eq. (4) to obtain all variable terms of the lattice energy.

To consider the relaxation effect on the NN-NNN bonding energies, we used a supercell consisting of 64 C atoms with

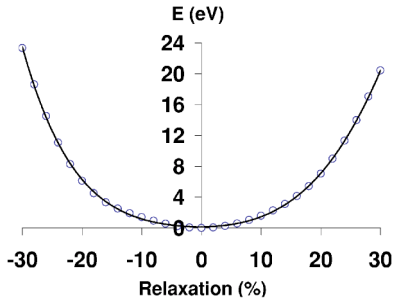

FIG. 2. The variation of elastic energy between NN and NNN atoms of the vacancy with the outward (positive) and inward (negative) relaxation.

a vacancy at its center. Periodic boundary conditions were imposed to the unit cell. Before starting to relax the NN atoms of the vacancy, we minimized energy of the supercell with respect to the length of C—C bond in the lattice. The optimum bond length was obtained 1.55 Å and its related energy was set as the reference or the zero of the lattice energy. The positions of all C atoms in the supercell were fixed and the NN atoms were moved symmetrically inward and outward from the vacant site. The total energy of the lattice was obtained for each outward and inward displacement of the NN atoms [based on the SW potential in Eq. (4)]. The results are summarized in Fig. 2.

III. RESULTS AND DISCUSSION

A. Relaxation effect on the total energy of the defect molecule

The calculation results for the variation of total energy of the defect molecule with respect to the inward and outward relaxations are summarized in Fig. 3.

As it is evident from this figure, the variations of the relative energies of the levels are large. For example, the energy of the dipole allowed transition GR1 increases by 0.1 eV for 1% increase in the outward relaxation. However, it is also evident from the figure that the variation is different for different electronic states of the vacancy. The energies of ^1E, $^3T_1$, $^1A_1$, and $^1T_2$ vary appreciably with the relaxation but at much lower rate than the high spin $^5A_2$ state. This suggests

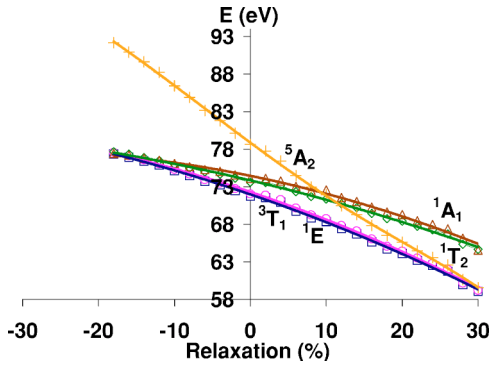

FIG. 3. (Color online) The variation of total energy of the defect molecule in different electronic states with the outward and inward relaxation.

that for obtaining proper quantitative results, the effect of the relaxation must be considered. This variation is much larger than the energy correction due to Jahn-Teller effect,[24] in agreement with the assumption of the previous CI calculation.[14] The important role of the lattice distortion in the optical character of Ni impurity in diamond was also demonstrated previously with a semiempirical CNDO calculation.[25]

In Fig. 3, in all ranges of the relaxation, the ground state remains ^1E and the position of the low lying excited state $^3T_1$ increases from 100 meV at −20% relaxation to 400 meV at +30% relaxation. In this wide range of relaxation, the position of the $^3T_1$ level is more than 100 meV above the ground state that is consistent with the suggestion made by EPR.[17] At 12% outward relaxation, there is a level crossing between the $^5A_2$ and $^1T_2$ that changes the order of these levels. The rapid energy decrease of the $^5A_2$ state with the outward relaxation, can explain for the first time the suggested midgap position for this state by EPR.[3] At 12% outward relaxation the ground state ^1E is about 3 eV below the crossing point of the $^5A_2$ and $^1T_2$ states, consistent with midgap energy of the diamond. Note that in the original CI model,[1] the position of this state has been found to be 5 eV above the ground state in the unrelaxed regime similar to findings at zero relaxation shown in Fig. 3.

The level crossing can explain the variation of the EPR signal with temperature. Vanwyk *et al.*[3] by increasing the temperature of the experiment and monitoring the EPR signal of the $^5A_2$ excited state of the V^0 at about 100 K, found that the $^5A_2$ state was excited with an activation energy of about 40 meV. They proposed that $^5A_2$ is about 40 meV below another short lived midgap state, more probably the $^1T_2$ state.

In this figure the energies vary almost linearly with respect to the relaxation with a negative slope. Therefore the outward and inward relaxation decreases and increases the total energy of the defect molecule, respectively. This effect occurs in all of the investigated lowest levels in Fig. 3.

The slope of the energy gives the forces involved in the relaxation[14] which are different for the different states. Hence the energy levels can also be ordered as decreasing the forces involved in lattice relaxation as $^5A_2$, ^1E, $^3T_1$, $^1T_2$, $^1A_1$, where the relaxing force of the $^5A_2$ is significantly larger than the other states. This can result in different amounts of lattice relaxation in different many electron states. In the $^5A_2$ state the decrease of the repulsive potential energy between NN bare ions (e^2/R) with the outward relaxation strengthen with the simultaneous decrease of the electronic energy between four half-filled dangling orbitals. This suggests that the relaxation for the high spin lattice vacancies which obey Hund rule should be outward. The different behavior of the levels under relaxation is understandable from electronic configurations in these states that will be explained in the next section.

In summary, results of Fig. 3 indicate that considering ion-ion interaction for the total energy of the defect molecule is essential to obtain the outward relaxation. The order of levels in increasing energy are as ^1E, $^3T_1$, $^1T_2$, $^1A_1$, and $^5A_2$, while with more than 12% outward relaxation the order changes to ^1E, $^3T_1$, $^5A_2$, $^1T_2$, and $^1A_1$.

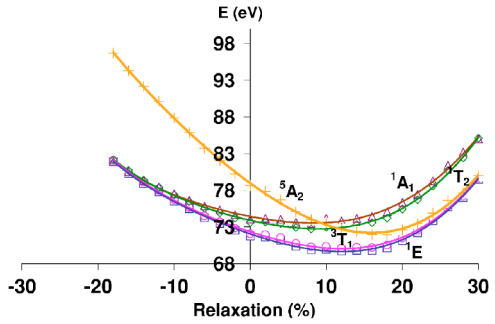

FIG. 4. (Color online) The variation of total energy of the vacancy in lattice, in different electronic state with the outward and inward relaxation.

B. Relaxation effect on the energies of the vacancy in lattice

Now we consider all energy terms involving relaxation of a vacancy in the lattice. For this purpose, we add the variation of the NN-NNN interaction energy (Fig. 2) to the variation of the total energy of the defect molecule (Fig. 3). The results are summarized in Fig. 4. As we observed in Fig. 3, considering ion-ion interaction results in an outward relaxing force for all electronic states. The outward relaxation continues until the elastic barrier due to NN-NNN interaction (Fig. 2) exceeds. This restricts the outward relaxation for each electronic state to a definite value.

In Fig. 4, for each electronic state, we obtained a minimum in the total energy curve for a definite size of the outward relaxation. Hence, the calculations give an outward symmetric displacement of the vacancy atoms in all of the electronic states. The results give 12% outward relaxation for the ground state ^1E as well as for the low-lying excited state $^3T_1$. The latter is predicted as the ground state in LDA-DFT calculations. Our obtained value for the relaxation size of the $^3T_1$ is in very good agreement with the results of *ab initio* DFT calculations.[5] The calculated size of the outward relaxation for the $^5A_2$ excited state in Fig. 4 is 18% and higher than the relaxation in the ground state. This is in good agreement with the 15% outward relaxation suggested by EPR[3] for the $^5A_2$. The amount of the relaxation for this state is also higher than the other states. The size of the relaxation for the excited state of the GR1 optical band, $^1T_2$, and also the $^1A_1$ state is 8%. The different size of lattice relaxation in different electronic states, is understandable from a very short lifetime of the lattice phonon that is about 10^{-14} s. This relaxation time is much shorter than the relaxation lifetimes of different electronic excitations. The lifetimes of electronic excitations are of the order of 1 ns (Ref. 9) for $^1T_2$ and 1 ms (Ref. 3) for $^5A_2$ indicating that during electronic relaxation, the ions will have enough time to relax to their new equilibrium configuration. Note that from the strengths of the vibronic coupling it is known that the bond lengths may differ by about 5% in different electronic states.[9] The calculation results in Fig. 4 gives a difference between 4% to 10% in the bond length in different electronic states corresponding to 8% relaxation for $^1T_2$ and 18% for $^5A_2$.

C. Electronic configurations

In this section using electronic configurations of the states, we explain the findings concerning the behavior of the vacancy electronic states under relaxation. For this purpose, we calculated many electron eigenfunctions of Eq. (2) for different relaxations. At first we present electronic configurations in the unrelaxed states and then we discuss the population variation of the electronic configurations with the relaxation.

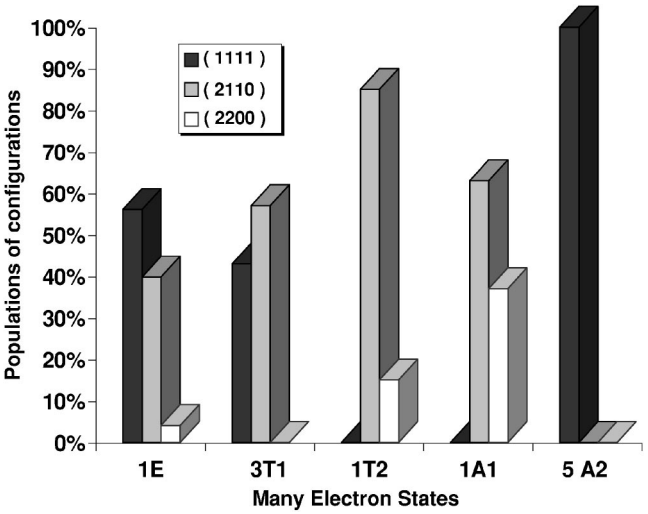

FIG. 5. Populations of available electronic configurations in the ground state and lowest electronic excitations of the unrelaxed vacancy. Numbers in parentheses are occupation numbers of each atomic orbital of the vacancy.

1. Electronic configurations in unrelaxed states

The usage of atomic orbital basis in the generalized Hubbard model enabled us to obtain new information about the quantum configurations of each unrelaxed electronic state. The basis is more natural than the previously used molecular basis[1] in describing physical properties of the system such as behavior of the Hund configuration of the $^5A_2$ state and also ionization of the vacancy atoms. The contribution of each allowed electronic configuration in the ground and the lowest excited states of the vacancy are summarized in Fig. 5. The numbers in parentheses in Fig. 5 are the occupation numbers of each vacancy atomic orbital. The ground state is spin singlet hence all of the possible orbital occupations are allowed. These allowed electronic configurations are (1,1,1,1), (2,1,1,0), and (2,2,0,0).

From Fig. 5, it is evident that the trend of the eigenstates is the growth of the paired configurations (2,1,1,0) and (2,2,0,0) relative to the Hund one (1,1,1,1) in going from lower to higher excited states. For higher excited states, we observe a growth of the doubly paired configurations with respect to the singly paired one. The Hund configuration is dominant in the ground state ^1E and disappears after few excitations. This trend has an interesting consequence. In going to the more excited states, there is a tendency to go toward the paired configuration. This means that at higher excited states the probability of finding states with a high value of spin decreases. In our calculation among the eight upper-half excited states of the vacancy, six states have zero spin (singlet) and two are triplet ($S=1$), and none of them

has $S=2$. Similar evidence can be obtained from the reported excited states in the Coulson and Kearsley model.[1]

The ground state ^1E has mainly (1,1,1,1) configuration (56%), where all of the vacancy atomic orbitals are half-filled. This means that the probability of finding the Hund configuration (1,1,1,1) in the ground state of the vacancy is 56%. The contribution of the paired configuration, (2,1,1,0) is appreciably 40%. As we expect, the contribution of the high energy or the double paired configuration (2,2,0,0) in the ground state is negligible (4%).

The 56% population for Hund configuration is consistent with Lannoo and Bourgoin[26] explanation for moderately correlated electrons of the diamond vacancy and Coulson and Kearsley remark,[1] "…when the constituent atoms are farther apart than in a normal molecule we may not apply the Hund rule without careful consideration."

The $^5A_2$ excited state of the vacancy consists purely of the (1,1,1,1) configuration which is about 6 eV above the ground state ^1E in the unrelaxed regime (Fig. 3). Significant contribution of the paired configuration (2,1,1,0) reduces the energy of the ^1E state relative to the $^5A_2$ in zero relaxation (Fig. 3). Unlike in silicon, where Jahn-Teller effect is needed for reducing the ground state energy after electron pairing, there is no report on significant static Jahn-Teller effect in the ground state of the diamond vacancy.[8] This suggests that the energy reduction by pairing should have a pure electronic character in the diamond vacancy.

The calculation results show that in the two regimes the excited $^5A_2$ state can be the ground state of the vacancy. The first is in the free atom or weakly correlated limit[26,27] where the kinetic energy of electrons increases and the single electron parameter t of Eq. (2) becomes more effective than the correlation parameters such as U. The second regime is the strongly correlated limit, where the value of the one-site Coulomb interaction parameter U becomes much higher (about 7 times in our calculation) than the kinetic energy. In this regime, the electron pairing extremely increases the energy of the system and the ground state favors purely the (1,1,1,1) configuration.

As it is evident from Fig. 3, the $^3T_1$ state is very close to the ground state ^1E. The model explains this according to the similar electronic configurations of these two states in Fig. 5. The $^3T_1$ consist of 43% (1,1,1,1) and 57% (2,1,1,0) compared to 56% (1,1,1,1) and 40% (2,1,1,0) for the ^1E. It seems that the pairing for the ^1E is more effective than $^3T_1$ in reducing the energy of the state. It can be concluded that the mixing of the paired configuration with the Hund one reduces the energy of the state until the contribution of the paired configuration exceeds the Hund configuration. By neglecting the orbital overlap parameter s, the hopping parameter t_{ij} will be zero. With this value our calculation reproduces the previous result of the original CI calculations[1] and the position of the $^3T_1$ will be 50 meV above the ground state.

For the first dipole allowed excited state $^1T_2$, the model predicts 85% (2,1,1,0) and 15% (2,2,0,0). The contribution of the allowed (1,1,1,1) is absolutely zero. From these results we can summarize the change of the electronic configurations, via the GR1 transition as

$$\text{GR1:}\quad (1,1,1,1)+\hbar\omega \rightarrow 0.8(2,1,1,0)+0.2(2,2,0,0). \tag{5}$$

This shows photon absorption at 1.673 eV (GR1) changes the Hund configuration to the paired ones. The probability of finding semipaired configuration (2,1,1,0) in the excited state is four times of finding full paired (2,2,0,0) configuration. The Eq. (5) also explains the strong dependence of the calculated value of the GR1 transition energy to the energy increase of the system due to pairing, i.e., U, in previous molecular models.[1,28,29]

From Fig. 5 we find that, the wave function of the ground state of GR1 is distributed on all of the allowed configurations. Equation. (5) demonstrate that the main contribution in the ground state (1,1,1,1) will change to other configurations in the excited state of the dipole allowed GR1 transition. This reduces significantly the overlap integral of the ground and excited states wave functions and the related dipole transition intensity of the GR1 transition. It should be noted that the lowest value of the spin for the GR1 transition plays a fundamental role in such effect. This is unlike the high spin transitions in which the Hund rule can be applied to their ground states. One example, is the dipole allowed transition in the negatively charged vacancy (V^-), i.e., ND1 transition. The maximum spin value of the ground state in such transition, restricts the electronic configurations of the ground and excited state to a common and allowed configuration which has a minimum number of paired electrons. For ND1 the ground and excited states belong to the (2,1,1,1) configuration due to the maximum value of the spin $S=\frac{3}{2}$. This increases the overlap integral of the dipole transition amplitude, and also the related dipole transition intensity. This is in agreement with the optical spectroscopy data that obtains dipole transition intensity of ND1 about four times higher than GR1.[30,31] This picture has been extended[32] to the experimental data about relative oscillator strength of the other low spin color centers in diamond such as N-V, N3, H3, and H4 which have much lower oscillator strengths than V^-.

Let us discuss about the EPR observation of $^5A_2$ in diamond samples that contain V^- (type IaB) during illumination of the UV light.[3] Based on Hund configuration of the ND1 transition, our model explains the ionization of the V^- and the resultant state of the neutral vacancy (V^0). Following previous molecular orbital calculations,[29] we obtained

$$\begin{aligned}(2,1,1,1)(V^-)+\hbar\omega &\rightarrow (2,1,1,1)*(V^-)\\ &\rightarrow (1,1,1,1)(V^0)+e^-.\end{aligned} \tag{6}$$

This relation demonstrates that in the photon absorption process, there is no configuration change and the energy of the configuration increases by 3.159 eV. This highly excited state is unstable and can relax by ejecting its more energetic electron, i.e., one of the paired electrons. The resultant configuration is (1,1,1,1) which is a pure Hund configuration that represents the $^5A_2$ state. Based on spin conservation rule, in the mentioned ionization process, the resultant states of the V^0 should have a spin value equal to 2 or 1. Among five lowest states of the V^0 only $^3T_1$ and $^5A_2$ have such spin values. EPR has detected $^5A_2$ but suggests a fraction of the

V^- ionize to this state.[3] Our calculation favors (1,1,1,1) configuration after the ionization process and suggests the $^5A_2$ as the more probable final state. The previously used[1] molecular a^2t^3 configuration for the ND1 states favors[3] other available states with (2,1,1,0) configuration such as $^3T_1$. Equation (6) is consistent with the EPR experiment[3] and nonluminescence result of the ND1.[16,17] This has been associated with a transition from $^4T_1$ excited state of the V^- to the $^5A_2$ excited state of the V^0.

2. Effect of the lattice relaxation on electronic configurations

As we observed in Fig. 5, the many electron states of the vacancy are a mixture of the (1,1,1,1), (2,1,1,0), and (2,2,0,0) configurations. We expect that the (1,1,1,1) configuration is more sensitive than others to the size of the relaxation. In this configuration the relative distance of four electrons that are attached to the four dangling orbitals changes maximally with the relaxation. This is unlike the (2,2,0,0) configuration, in which we expect that the relaxation does not affect significantly the electronic energy.

The (1,1,1,1) configuration of the $^5A_2$ explained the strong dependence of this state on the lattice relaxation in Fig. 3 and its related maximum relaxing force. In going from the inward to outward relaxation, the ionic distance (R) and hence the related dangling orbitals of NN atoms will be farther apart from each other. This decreases both ionic and electronic interaction repulsion energies. The latter are represented by the multicenter *e-e* interaction parameters of Eq. (3). As we showed in Fig. 5, the calculation results give almost equal weight for the (1,1,1,1) and (2,1,1,0) configurations in the ground state ^1E and the low-lying $^3T_1$ state. The paired configurations introduce U to the *e-e* interaction energy which its value is independent from the relaxation. Such mixed states show less dependence to the relaxation with respect to a pure (1,1,1,1) configuration, i.e., $^5A_2$ state. The electronic configurations in the excited state of the GR1 absorption band $^1T_2$ and also $^1A_1$ are much different from the $^5A_2$. They are a mixture of the paired configurations (2,1,1,0) and (2,2,0,0) and does not contain any (1,1,1,1) configuration (Fig. 5). This explains similar behavior of these states under relaxation in Figs. 3 and 4. As we expect, the energy reduction of these states by outward relaxation and also the related relaxing force is the lowest (Fig. 3).

We have also calculated the effect of the outward and inward relaxation on the populations of the different electronic configurations in each state. The populations of configurations in the equilibrium positions of NN atoms in each electronic states are shown in Fig. 6. For comparison we have also shown similar results at 12% inward relaxation in Fig. 7.

By outward relaxation, the energy of the (1,1,1,1) configuration decreases more rapidly than the (2,1,1,0) and (2,2,0,0) configurations. As it is evident in Fig. 6, by outward relaxation, the population of (1,1,1,1) configuration increases in comparison to the paired configurations in each many electron state. In the ground state the population of (1,1,1,1) increases from 56% in the unrelaxed vacancy to 70% in 12% outward relaxed vacancy. In the low lying $^3T_1$ state we also observe an increase from 43% to 65% for the population of the (1,1,1,1) configuration. Simultaneously, there is a reduction in the population of the paired (2,1,1,0) and (2,2,0,0) configurations with outward relaxation. This reduction is from 40% to 28% and also from 57% to 35% for ^1E and $^3T_1$ states, respectively.

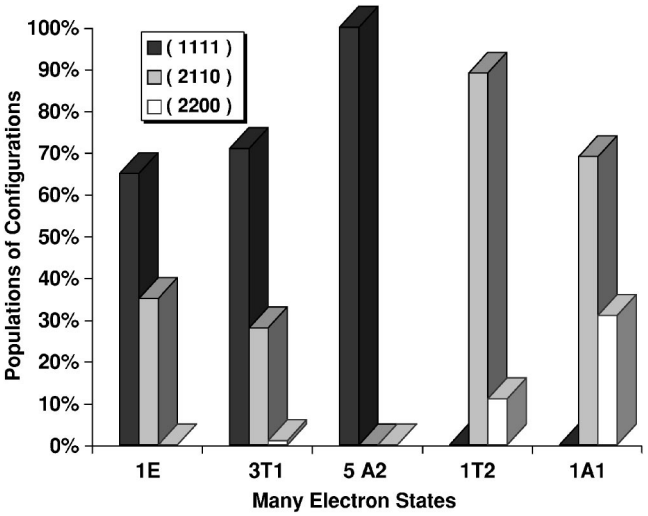

FIG. 6. Populations of available electronic configurations for ^1E and $^3T_1$ at 12% outward relaxation and for $^1T_2$ and $^1A_1$ at 8% outward relaxation. Numbers in parentheses are occupation numbers of each atomic orbital of the vacancy.

The proposed picture explains why the level crossing only occurs between the $^5A_2$ and $^1T_2$ ($^1A_1$) levels in the investigated relaxation range of Fig. 3. Among all of the many electron states, only these two have no common electronic configuration. While the $^5A_2$ has only (1,1,1,1) configuration, the $^1T_2$ and $^1A_1$ consist completely of the paired configurations (2,1,1,0) and (2,2,0,0). By population variation with outward relaxation, these two states cannot reach to a common configuration and its related common energy. Therefore

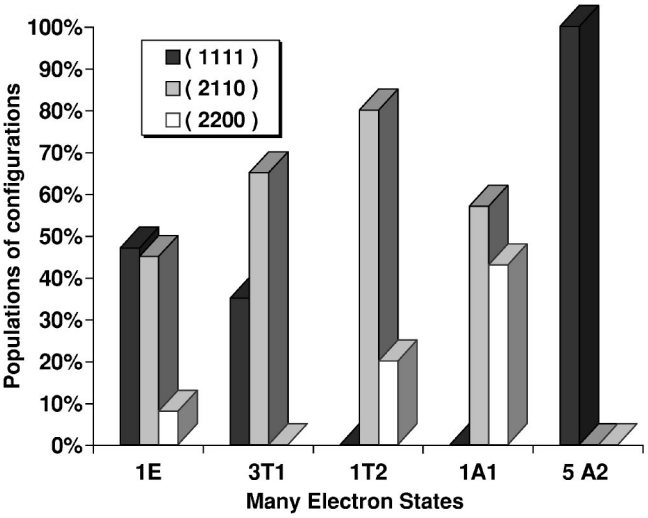

FIG. 7. Populations of available electronic configurations in the ground state and lowest electronic excitations of the 12% inward relaxed vacancy. Numbers in parentheses are occupation numbers of each atomic orbital of the vacancy.

we found a level crossing between these two states. This is unlike the behavior of the ^1E and $^3T_1$ states which have common (1,1,1,1) configuration with the $^5A_2$. As it can be observed in Figs. 3 and 4, ^1E, $^3T_1$, and $^5A_2$ converge to a common energy for extremely outward relaxations (+30%). This is associated with their common (1,1,1,1) configuration. At this limit, the completely paired states $^1T_2$ and $^1A_1$ which have no (1,1,1,1) contribution diverge.

For the inward relaxation, the (1,1,1,1) configuration has the largest rate of energy increase with relaxation and also related relaxing force. The paired configurations are less sensitive to the size of the inward relaxation. In going from unrelaxed to the more inward relaxed states we encounter a decrease in the population of the (1,1,1,1) in favor of an increase in the population of the paired configurations (Fig. 7). We found a reduction of (1,1,1,1) configuration from 56% to 47% and 43% to 35% for the ^1E and $^3T_1$ states at 12% inward relaxation, respectively. As we expect, by increasing the inward relaxation all of the lowest levels go toward configuration with more paired electrons and with less Hund configuration. This explains the behavior of the states under extreme size of the inward relaxation (−20%) in Figs. 3 and 4. In these figures the low lying states ^1E and $^3T_1$, that have common paired configurations (2,1,1,0) and (2,2,0,0) lose their (1,1,1,1) configuration with the inward relaxation and converge to a common configuration with its related common energy. These configurations exist also in the $^1T_2$ and $^1A_1$ states that have no (1,1,1,1) configuration. The energy of the $^5A_2$ state that has only (1,1,1,1) configuration increases by inward relaxation and is appreciably higher than the common energy of the other states in the extreme inward relaxation (−20%) limit.

In summary, with outward relaxation, the electronic configurations in many electron states become more Hund type and with inward relaxation, the states become more paired-like.

IV. CONCLUSION

We investigated the lattice relaxation effect in many electron states of the diamond vacancy. The generalized Hubbard Hamiltonian was used to calculate *e-e* interaction energy accurately in each relaxed configuration of the NN atoms. The interaction of the first and second shell neighbors (NN—NNN) was calculated with the SW potential. We demonstrated that the energy correction due to the lattice relaxation around a vacancy is much higher than the correction of the Jahn-Teller distortion. Results indicate that considering the role of this effect is vital in order to calculate the energies of electronic excitations. The order of the investigated states and particularly the ground state ^1E do not change under relaxation and the low lying $^3T_1$ state is more than 100 meV above the ^1E in all of the investigated range. A level crossing between the $^5A_2$ and $^1T_2$ was observed at 12% outward relaxation. By considering the ion-ion interaction term, we found that all of the levels favor outward relaxation with different relaxing force. The relaxing force for the high spin state $^5A_2$ is higher than the other states. Including the elastic barrier of the NN—NNN interaction into the calculations, the final symmetric configuration of the NN atoms was obtained in each electronic states. The relaxation size for the ground state ^1E and the low-lying excited state $^3T_1$ is 12%, in very good agreement with the results of the *ab initio* DFT calculation results. The relaxation size for the high spin excited state $^5A_2$ was obtained to be 18%, in good agreement with the EPR measurement results. The relaxation in the $^1A_1$ and $^1T_2$ states were also obtained to be 8%. The calculated electronic configurations in the unrelaxed states were discussed. Using variation of the electronic configurations with the lattice relaxation, we explained different behavior of the energy levels under inward and outward relaxation and also the origin of the level crossing. During outward and inward relaxations, electronic configurations become more Hund-type and paired-like, respectively. The model predicts outward relaxation for a high spin vacancy in which the Hund rule is applicable.

Using *ab initio* LDA orbitals for calculating parameters of the generalized Hubbard Hamiltonian is under consideration. By this means, the model can investigate symmetric lattice relaxation in different charged states of the vacancy in diamond and other semiconductors.

ACKNOWLEDGMENTS

We would like to thank Professor J. M. Baker and Dr. J. P. Goss for their discussions.

[1] C. A. Coulson and M. J. Kearsley, Proc. R. Soc. London **241**, 433 (1957).
[2] G. D. Watkins, in *Deep Centers in Semiconductors*, 2nd ed., edited by S. T. Pantelides (Gordon and Breach, New York, 1992), p. 177.
[3] J. A. Vanwyk, O. D. Tucker, M. E. Newton, J. M. Baker, G. S. Woods, and P. Spear, Phys. Rev. B **52**, 12657 (1995).
[4] J. Isoya, H. Kanda, Y. Uchida, S. C. Lawson, S. Yamasaki, H. Itoh, and Y. Morita, Phys. Rev. B **45**, 1436 (1992).
[5] S. J. Breuer and P. R. Briddon, Phys. Rev. B **51**, 6984 (1995).
[6] A. Zywietz, J. Furthmuller, and F. Bechstedt, Phys. Status Solidi B **210**, 13 (1998).
[7] U. Gerstmann, M. Amkreutz, and H. Overhof, Phys. Rev. B **60**, R8446 (1999).
[8] U. Gerstmann and H. Overhof, Physica B **308**, 561 (2001).
[9] G. Davies, in *Properties, Growth and Application of Diamond*, edited by M. H. Nazare and A. J. Neves (IEE, London 2001), p. 193.
[10] J. E. Lowther, in *Properties, Growth and Application of Diamond*, edited by M. H. Nazare and A. J. Neves (IEE, London 2001), p. 179.
[11] R. P. Messmer and G. D. Watkins, Phys. Rev. B **7**, 2568 (1973).

[12] A. Mainwood, J. Phys. C **12**, 2443 (1979).
[13] L. H. Li and J. E. Lowther, Phys. Rev. B **7**, 2568 (1973).
[14] C. A. Coulson and F. P. Larkins, J. Phys. Chem. Solids **32**, 2245 (1971).
[15] G. Davies, Rep. Prog. Phys. **44**, 787 (1981).
[16] G. Davies and N. B. Manson, in *Properties and Growth of Diamond*, edited by G. Davies (IEE, London 1994), p. 159.
[17] D. J. Twitchen, M. E. Newton, M. Baker, and V. A. Nadolinny, in *Properties, Growth and Application of Diamond*, edited by M. H. Nazare and A. J. Neves (IEE, London 2001), p. 214.
[18] M. Heidari Saani, M. A. Vesaghi, K. Esfarjani, and A. Shafiekhani, Diamond Relat. Mater. **13**, 2125 (2004).
[19] F. H. Stillinger and T. A. Weber, Phys. Rev. B **31**, 5262 (1985).
[20] J. Tersoff, Phys. Rev. Lett. **61**, 2879 (1988).
[21] D. W. Brenner, Phys. Rev. B **42**, 9458 (1990).
[22] A. S. Barnard and S. P. Russo, Mol. Phys. **100**, 1517 (2002).
[23] A. S. Barnard, S. P. Russo, and G. I. Leach, Mol. Simul. **28**, 261 (2002).
[24] M. Lannoo and A. M. Stoneham, J. Phys. Chem. Solids **29**, 1987 (1968).
[25] L. Paslovsky and J. E. Lowther, J. Phys. Chem. Solids **54**, 243 (1992).
[26] M. Lannoo and J. Bourgoin, in *Point Defects in Semiconductors, I, Theoretical Aspects* (Springer, Berlin, 1981), p. 141.
[27] A. M. Stoneham, in *Defects in Crystals* (Springer, Berlin, 1981), p. 141.
[28] J. E. Lowther, Phys. Rev. B **48**, 11592 (1993).
[29] A. Mainwood and A. M. Stoneham, J. Phys.: Condens. Matter **9**, 2453 (1997).
[30] G. Davies, Physica B **273–274**, 15 (1999).
[31] G. Davies, S. C. Lawson, A. T. Collins, A. Mainwood, and S. J. Sharp, Phys. Rev. B **46**, 13157 (1992).
[32] M. Heidari Saani, M. A. Vesaghi, and K. Esfarjani, Eur. Phys. J. B **39**, 441 (2004).